Publ. Astron. Soc. Japan, **41**, 809–822 (1989)

Continuum Observations of M17, W49 A, and W51 A at 43 GHz*

Kenji AKABANE

Department of Physics, Faculty of Science, Toyama University, 3190, Gofuku, Toyama 930

Yoshiaki SOFUE

Institute of Astronomy, The University of Tokyo, Mitaka, Tokyo 181

Hisashi HIRABAYASHI

Institute of Space and Astronautical Science, 1-1, Yoshinodai 3-chome, Sagamihara-shi, Kanagawa 229

and

Makoto INOUE

Nobeyama Radio Observatory, Minamimaki-mura, Minamisaku-gun, Nagano 384-13

(Received 1988 July 29; accepted 1989 January 23)

Abstract

In this paper 43.3-GHz continuum observations of the galactic H II regions M17, W49 A, and W51 A are presented. Observations were made with a single-dish of 39″ resolution, and the contour maps were compared with those of 3-mm wavelength results by Gordon et al. (1986; AAA 42.132.029). Each resolved area of the sources essentially shows a fairly reasonable thermal spectrum, though there is a weak millimeter-wave intensity excess in the near-south diffuse area of the M17 S-bar. An unfilled concentration of extremely compact and high-density ionized condensations is suggested in this highly obscured area of M17. In comparison with the Fleurs 1415-MHz map of M17, the self-absorption of the ionized region seems to be more effective in the surrounding edge of the sources than in the central peak area of the region. A morphological similarity between W49 A and W51 A is shown.

Key words: H II regions; Interstellar medium; Radio continuum.

1. Introduction

Single-dish observations of the galactic H II regions M17, W49 A, and W51 A with

* Based on observations made at the Nobeyama Radio Observatory (NRO). NRO is a branch of the National Astronomical Observatory, an inter-university research institute operated by the Ministry of Education, Science, and Culture.

a resolution higher than 1′ in the short centimeter-wavelength region have not yet been made, except for a survey of the galactic H II regions by Gordon et al. (1986) with a resolution of 63″ or 70″. They concluded that no dust emission was observed in the 3-mm wavelength region, and have successively found clear dust emission of the galactic H II regions in the 1.3-mm wavelength region (Gordon 1987).

High-resolution interferometer (the One-mile telescope) observations were made for the W49 region by Wynn-Williams (1969) in the decimeter wavelength region; W49 A was resolved into two components. Three or more resolved components were reported in the main area of W51 A with the same telescope by Martin (1972), though in the centimeter wavelength region. These rather low-frequency but high-resolution (several 10″) results, based upon a nearly full-aperture synthesis, are to be compared with the new high-resolution single-dish results in the short centimeter and millimeter wave regions, and must be quite useful in determining the intensity spectrum within a wide range of frequencies for individual resolved sources.

Radio interferometer maps of the free-free emission from M17 were reported by Webster et al. (1971), Löbert and Goss (1978), Matthews et al. (1979), Felli et al. (1980), and Felli et al. (1984). Of these, a Fleurs 1.415-GHz map was obtained with a nearly full aperture synthesis, where a grating interferometer (Christiansen Cross) was employed, though the system was modified to two-aperture synthesis interferometers (FST) without missing the interferometer spacing, at least down to the solar diameter. Therefore, the single-dish observational results can be reasonably compared with the Fleurs map, even though the resolution is not so high.

VLA maps of M17 at the 21- and 6-cm wavelengths were reported by Felli et al. (1984); they found a complicated fine structure of many outstanding compact condensations of 1″ to 10″, establishing a radio patchy complex structure of the galactic H II regions.

The aim of this continuum study is to investigate the nature of the homgeneity of the H II regions. The intensity spectral index for parts of the region is derived in order to detect any optically thick component if it exists there.

An optically thick area in the region will give an increasing flux density with increasing frequency, even though the main part of the region should show an exactly thermal flat spectrum. An excess intensity in the high-frequency region may suggest an unfilled collective structure of extremely high-density compact H II condensations in a homogeneous optically thin ionized medium.

For the Ori A and W3 regions, millimeter wave observations for this scheme were made and the possible existence of some millimeter-wave intensity excess was reported by Akabane et al. (1985, 1986). Recently, a millimeter-wave intensity decrease was reported which was attributed to a nonthermal source in the thermal region of the Sgr B2 south region (Akabane et al. 1988).

2. Observations

On April 30, 1985, 43-GHz observations of the regions M17, W49 A and W51 A were made as one part of a radio continuum survey of galactic sources at NRO. We used the NRO 45-m telescope equipped with a Schottky-barrier diode-mixer receiver

combined with a parametric amplifier, both being He-cooled at the 20K stage. The center frequency and bandwidth were 43.25 and 0.5 GHz, respectively. The system temperature was about 500 K at the zenith. One linear polarization was detected, and was fixed with each elevation angle of the telescope. For observations of M17 and W51 A a beam-switching mode was employed in which the main beam was switched at a frequency of about 20 Hz to a wide reference beam separated by about 8° in the azimuth direction from the main beam axis. For observation of W49 A another reference beam was used which had an almost identical beamwidth to that of the main beam and separated by 6′ in the azimuth direction from the main beam axis of the telescope. The new type of beam switching system of the NRO 45-m telescope will be described in a forthcoming paper by M. Inoue et al.

Pointing calibrations and checking of the beam switching responses were made by observing the source 3C 273 at the start of an observation. The pointing accuracy was estimated to be less than $\pm 15''$ in the mapping regions. A 39″ almost circular beam was obtained at the half maximum of the main beam. The major side lobes were found to be below -20 dB of the top of the main beam. A flux calibration was made while referring to the maps obtained with the source NGC 7027 just after an observation of the regions. The flux density of NGC 7027 at 43.25 GHz was taken to be 6.0 ± 0.3 Jy, similarly to the case of the observation of Sgr A region by Sofue et al. (1986), by extrapolating the spectrum determined by Harris and Scott (1976).

The mapping was carried out by scanning each region along the direction of right ascension every 15″ step of declination. The coverage of the mapping was $\Delta\alpha \times \Delta\delta = 24' \times 24'$ centered at $(\alpha, \delta) = (18\text{h}\,17\text{m}\,40.0\text{s}, -16°12'0'')$, $\Delta\alpha \times \Delta\delta = 5' \times 5'$ centered at $(\alpha, \delta) = (19\text{h}\,07\text{m}\,52.0\text{s}, 9°1'0'')$, and $\Delta\alpha \times \Delta\delta = 20' \times 20'$ centered at $(\alpha, \delta) = (19\text{h}\,24\text{m}\,26.2\text{s}, 14°24'43''.6)$ for the regions M17, W49 A, and W51 A, respectively. The observed peak brightnesses, T_{BP}, are 5.3 ± 0.5 K, 5.0 ± 0.5 K, and 8.7 ± 0.5 K at the peaks of M17 (S-bar top), W49 A, and W51 A, respectively, 1 K of T_{BP} corresponding to the brightness of 5.7×10^{-19} W m^{-2} Hz^{-1} sr^{-1} or 1.6 Jy/(39″ beam area). Confusion from the 43.12-GHz SiO maser line to the present observation was negligibly small, less than 0.002 K of T_B (N. Ukita, M. Ohishi, and T. Hasegawa; private communication).

The reduction of the 43-GHz data was performed by using the astronomical reduction system, CONDUCT, at NRO. The scanning effect on the map was removed by applying the pressing method developed by Sofue and Reich (1979).

3. Observational Results

3.1. M17 (W38)

Figure 1 shows the 43.3-GHz map of M17, in which the original 39″ resolution map was smoothed to a 45″ resolution so as to reduce the wind effects on the telescope during observations. The source is clearly resolved into a large-scale structure as M17 (a) and M17 (b) (Gordon et al. 1986) corresponding to S-bar and N-bar (Felli et al. 1984), respectively. In the present observation we distinguished two components, M17 (a1) and M17 (a2) (figure 1). A summary of the observational results is listed in table 1 along with the results of the 94.2-GHz map by Gordon et al. (1986), the 23.2-GHz

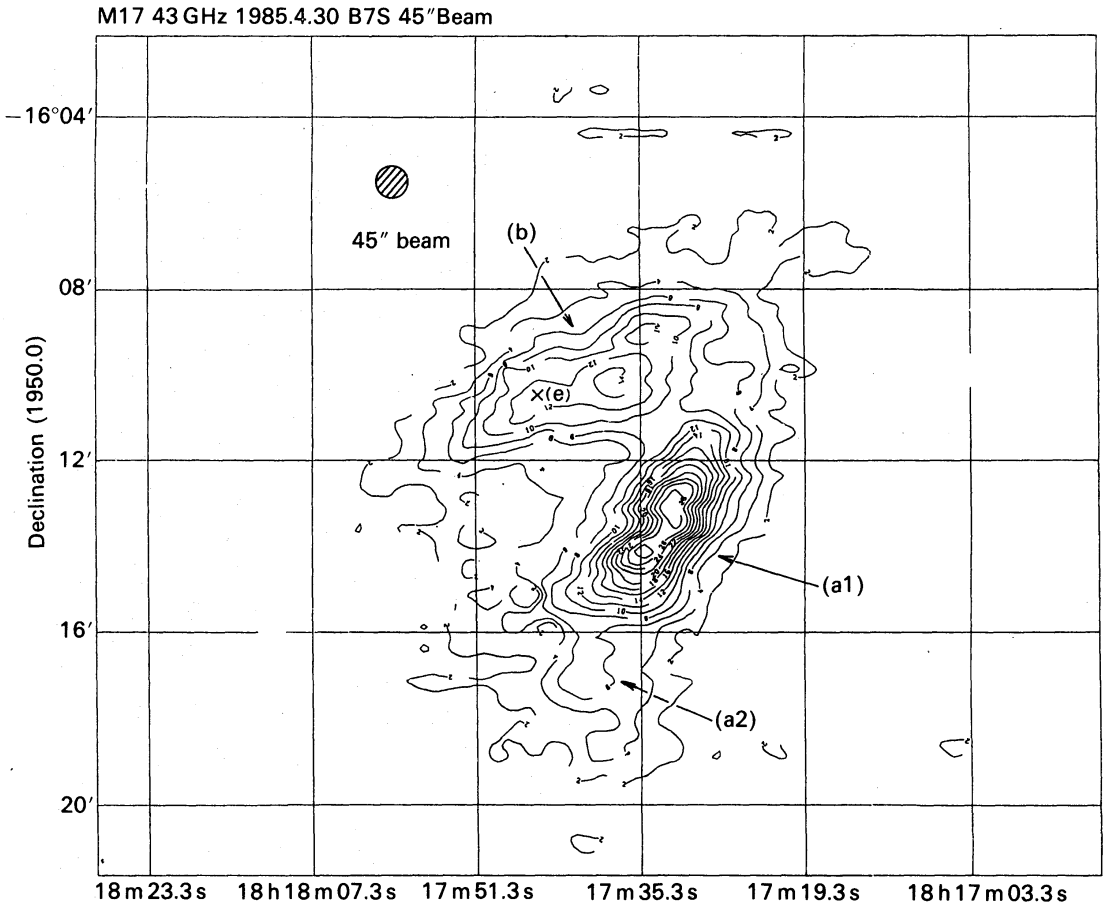

Fig. 1. 43.3-GHz map of M17. The top contour (S-bar peak) of the map corresponds to 5.3 K (±0.5 K) of the source T_B (brightness temperature). Components M17 (a1), M17 (a2), and M17 (b) are shown.

map by W. Reich and P. Reich (private communication) obtained with the NRO 45-m telescope, and the 1.415-GHz map by Löbert and Goss (1978). Flux densities S_ν and source extensions θ_s(max) and θ_s(min) of the components have been estimated from these short millimeter-wave, short centimeter-wave, and decimeter-wave original data, and are listed in table 1.

The new component, M17 (a2), is located at the south edge of the S-bar, and is a part of the S-bar, though the isolation from the main part is quite clear in both maps of $\lambda = 21$ cm and $\lambda = 6$ cm by Felli et al. (1984). A comparison of the 94.2- and 43.3-GHz intensities of M17 (a2) was made in the present study. The difference between two cross-cuts along AA′ in figure 3 is given in figure 2, and sguggests an excess of the 94.2-GHz intensity relative to that of 43.3 GHz in this area. Several cross-cuts, similar to those of figure 2, through region (a2) give a map of the 94.2-GHz relative excess brightness (figure 3), and a probable feature of the excess region is also given at the bottom of table 1.

In table 1, the 43.3- and 23.2-GHz flux densities of each component are larger than those at 94.2 GHz, though each total intensity may be strongly affected by the estimate of the extension of the zero contour level and, consequently, may be subject to a large

Table 1. Summary of the observational results of M17.

Physical	M17 (a1)	M17 (a2)	M17 (b)	Total
	S-bar		N-bar	
Peak position at 43.3 GHz:				
R.A. (1950.0)	$18^h17^m33^s$	$18^h17^m41^s$	$18^h17^m41^s$	...
Decl. (1950.0)	$-16°13'10''$	$-16°17'00''$	$-16°10'10''$	...
S_ν (Jy):				
94.2 GHz		239.4	144.6	384.0
43.3 GHz	207 ± 50	58 ± 20	218 ± 50	483 ± 90
23.2 GHz	194 ± 50	59 ± 20	213 ± 50	466 ± 80
Source size $\theta_s(\max) \times \theta_s(\min)$:				
94.2 GHz	$4'.2 \times 1'.6$	$(\sim 4') \times (\sim 4')$	$6'.2 \times 2'.4$	...
43.3 GHz	$4'.2 \times 1'.6$	$\sim 3'.2 \times \sim 3'.2$	$6'.2 \times 2'.4$	...
23.2 GHz	$4'.1 \times 1'.3$	$3'.2 \times 3'.2$	$6'.2 \times 2'.4$	...
1415 MHz	$4'.4 \times 1'.1$*	$\sim 3' \times \sim 3'$	$6'.5 \times 1'.6$*	...
94.2-GHz excess:				
Extent	...	$5' \times 2'.3$	...	...
Flux density	...	~ 28 Jy	...	...

Short millimeter-wave result (Gordon et al. 1986) and decimeter-wave result (Löbert and Goss 1978) of the region are also tabulated for a comparison with the present work.

Notes: 94.2-GHz results with beamwidth of 63″ by Gordon et al. (1968).
23.2-GHz results with beamwidth of 72″ by Reich and Reich (pivate communication).
1415-MHz results with beamwidth of 54″ × 48″ by Löbert and Goss (1978).
43.3-GHz results with beamwidth of 45″; present work.

observational error. The extension width of each area is roughly estimated as an elongated ellipse structure of the source. The effective full widths along the major and minor axes of each source, $\theta_s(\max)$ and $\theta_s(\min)$, are listed in the table, and were measured from the four frequency maps at 94.2, 43.3, 23.2, and 1.415 GHz. The effective source sizes, $\theta_s(\max)$ and $\theta_s(\min)$, were estimated simply as $\theta_s^2(\max)$ [or $\theta_s^2(\min)] = \theta_{obs}^2(\max)$ [or $\theta_{obs}^2(\min)] - \theta^2(\text{beam})$ in the present study. The source sizes of M17 (a1) and M17(b) are in good coincidence for three high-frequency results of 94.2, 43.3, and 23.2 GHz, but M17 (a2) shows a larger extension at 94.2 GHz than those at three other low frequencies. We also note here that the width of the S- and the N-bar, $\theta_s(\min)$, at 1.415 GHz are relatively narrower than those at three other higher frequencies, as are indicated by asterisks in the table.

3.2. *W49 A*

Figure 4 shows the 43.3-GHz map of W49 A with a 45″ resolution. The source is clearly resolved into two components, W49 (a) and W49 (b), as those observed by Gordon et al. (1986). A summary of the observational results is given in table 2 along with the 84.2-GHz results by Gordon et al. (1986). The flux density of each component is in fairly good coincidence for both frequencies. The intrinsic effective source sizes, θ_s, in the table (for the corresponding cross-cut directions shown in figure 4) were obtained from both maps. The extensions along each cross-cut direction almost coincide with each other for both the 43.3- and 84.2-GHz contours. However, the cross-cut profiles

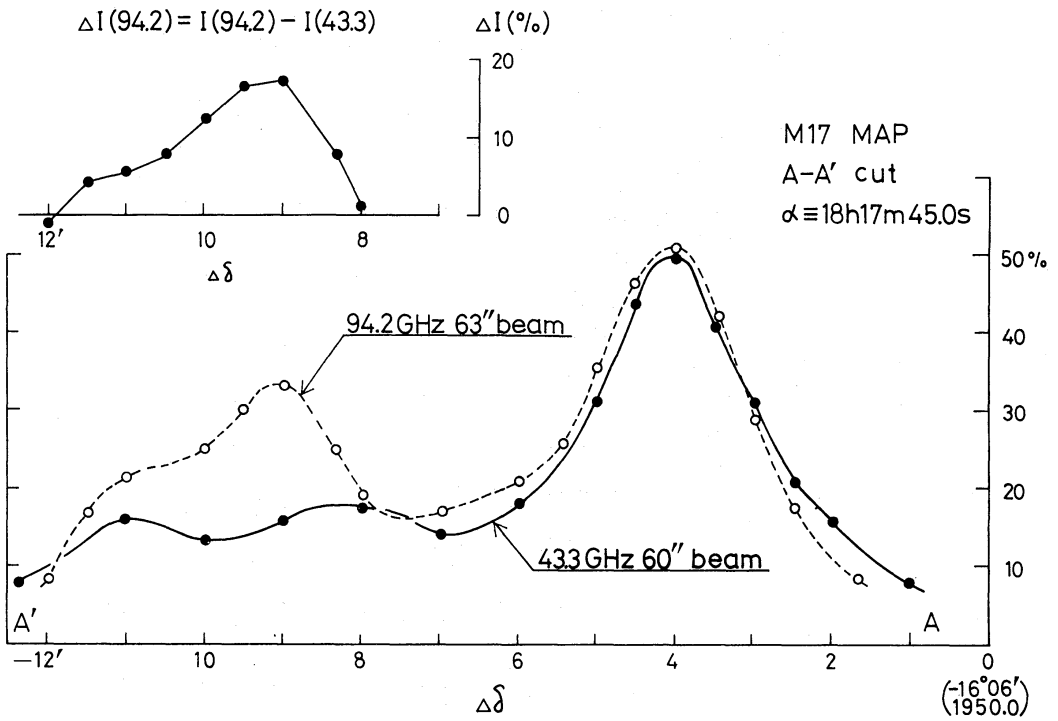

Fig. 2. Cross-cut profiles of the 43.3-GHz map of figure 3 and of the 94.2-GHz map by Gordon et al. (1986) along the AA′ line in figure 3. Both profiles in the figure are normalized at each top of the S-bar. For the profile at 43.3 GHz the map was reconvolved for 60″ resolution, which is almost the same as in the 94.2-GHz map (=63″) by Gordon et al. (1986). A comparison of the both cross-cut profiles is shown at the bottom, and the difference in these profiles is shown at the top-left of the figure.

along CC′ and DD′ in figure 4, show a possible excess extension of the source at 84.2 GHz, as indicated by asterisks in the table. In the direction of CC′ the main component W49 (a) has an extended component to the south west of the source as indicated by (a′) in figure 4, the excess width of which may lead to a millimeter-wave excess intensity relative to those at the centimeter-wave region. Along the DD′ cross-cut we also note a faint millimeter-wave excess width of the source.

Whereas W49 (b) appears to be unresolved, the extension at 84.2 GHz seems to be a little wider than those at 43.3 GHz, as shown in the cross-cut EE′ in table 2, suggesting the existence of weak millimeter-wave excess emission in the source.

3.3. W51 A

Figure 5 shows the 43.3-GHz map of W51 A with 45″ resolution. The source is clearly resolved into two components, W51 (a) and W51 (b), as observed at 84.2 GHz by Gordon et al. (1986). In the present observation the main part of source W51 (b) consists of at least two components, W51 (b1) and W51 (b2), as shown in figure 5. W51 (b1) is elongated in the BB′ direction in the figure and is hardly resolved to have a companion source to the north west of the region, as observed in previous interferometer studies by Martin (1972) and by Scott (1978) in the long centimeter-wave region.

Observational data of these components are summarized in table 3 with 84.2-GHz results for a comparison. The flux density of each component is in good agreement

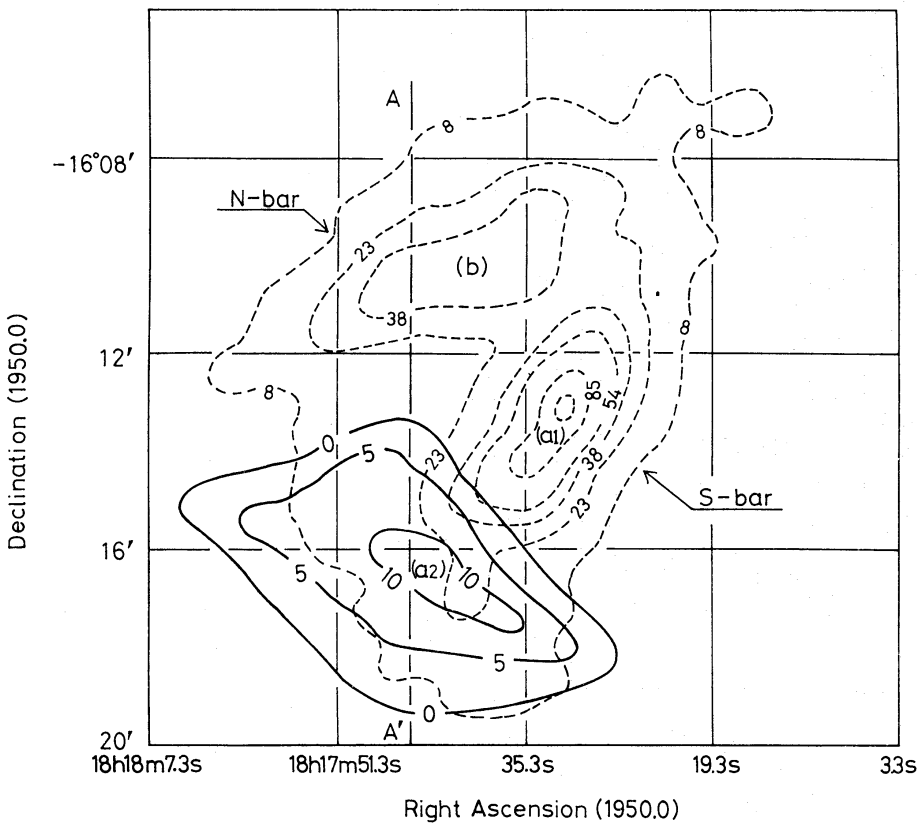

Fig. 3. The millimeter-wave excess in the M17 region. Solid line contours show a region of excess intensity at 94.2 GHz relative to that at 43.3 GHz. Dashed line contours are for the 60″ beam reconvolved 43.3-GHz map of M17. AA′ is the position of the cross-cut along right ascension (= 18h 17m 45.0s), profiles of which are shown in figure 2.

within observational errors. The intrinsic effective source sizes, θ_s, in the table, along each cross-cut (figure 5) were estimated from both maps. It can be seen in the table that source sizes of the components along each cross-cut profile are essentially the same for both frequencies. However, at 84.2 GHz a probable excess extension of the main source, W51 (b1), along the AA′ cross-cut can be noted, as indicated asterisks in the table, suggesting a 84.2-GHz excess emission relative to a thermal flat spectrum. A comparison of the two frequency cross-cuts along AA′ shows that an excess extension exists near the source edge between W51 (b1) and W51 (b2). For W51 (b2) another faint excess extension, also indicated by asterisk in the table, can be seen along the cross-cut CC′ in the figure. Hence a suggestion will be made that there exists a faint 84.2-GHz excess emission in the western extended area near W51 (b1) including W51 (b2).

4. Discussion

4.1. M17 (W38)

The M17 10-μm map by Kleinmann (1973) and the 21-μm map of M17 by Lemke and Low (1972) are all in good coincidence with the present radio map showing that the dust distribution in the region must be strongly associated with that of the ionized

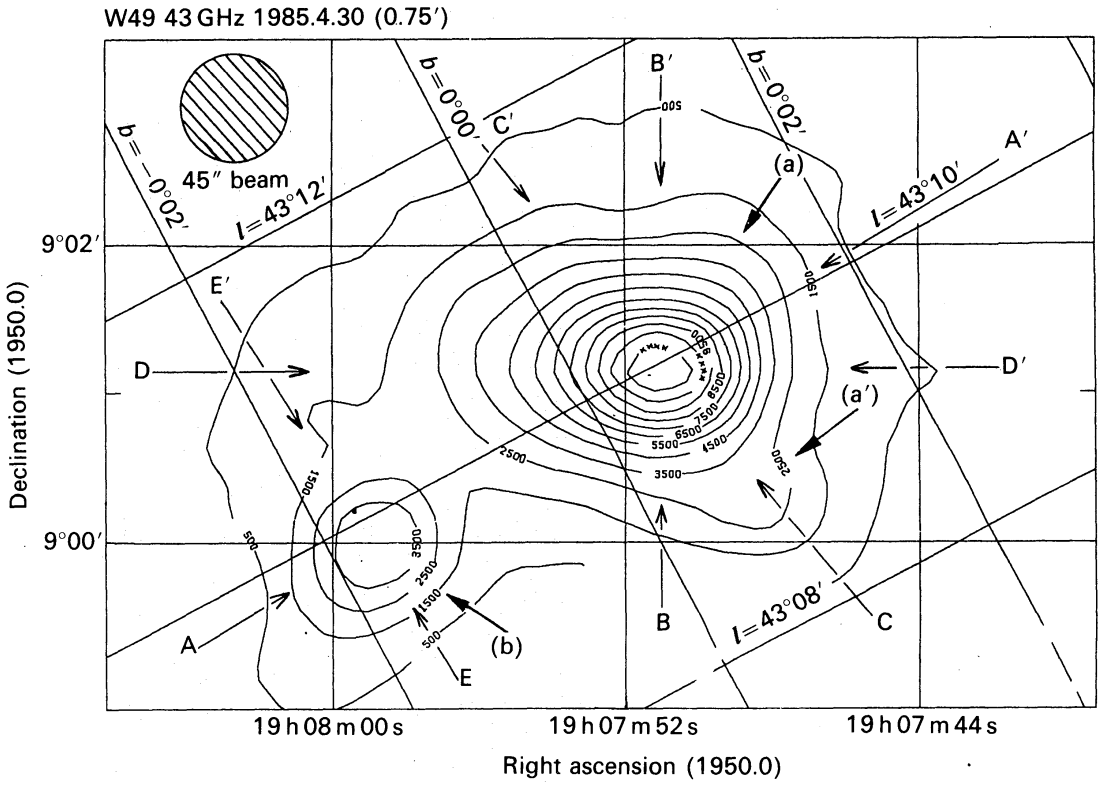

Fig. 4. 43.3-GHz map of W49 A. The top contour of the map corresponds to 5.0 K (±0.5 K) of the source T_B (brightness temperature). Arrows and marks AA′ etc, show the positions of each cross-cut through the contour map. Components W49 (a) and W49 (b) are shown.

Table 2. Summary of the observational results of W49 A.

	W49 (a)		W49 (b)		Total	
Peak position at 43.3 GHz:						
R.A. (1950.0)	$19^h07^m51^s$		$19^h07^m59^s$		...	
Decl. (1950.0)	+9°01′15″		+9°00′00″		...	
Frequency (GHz)	84.2	43.3	84.2	43.3	84.2	43.3
S_ν (Jy)	33.0	34.1±6	12.0	11.4±3	45.0	45.5±8
			Source size θ_s			
Cross-cut:						
AA′	0′.94	0′.89	0′.57	0′.49	...	...
BB′	0′.57	0′.58	...	...	...	...
CC′	0′.99*	0′.73	...	...	...	...
DD′	1′.23*	1′.06	...	...	...	...
EE′	...	...	0′.67	0′.45	...	...

The 84.2-GHz results of Gordon et al. (1986) are also reproduced in the table for a comparison with the present work. AA′ etc. in the table are marked in figure 4, showing the position of each cross-cut through the source.

Beamwidth: 70″ at 84.2 GHz (Gordon et al. 1986) and 45″ at 43.3 GHz.

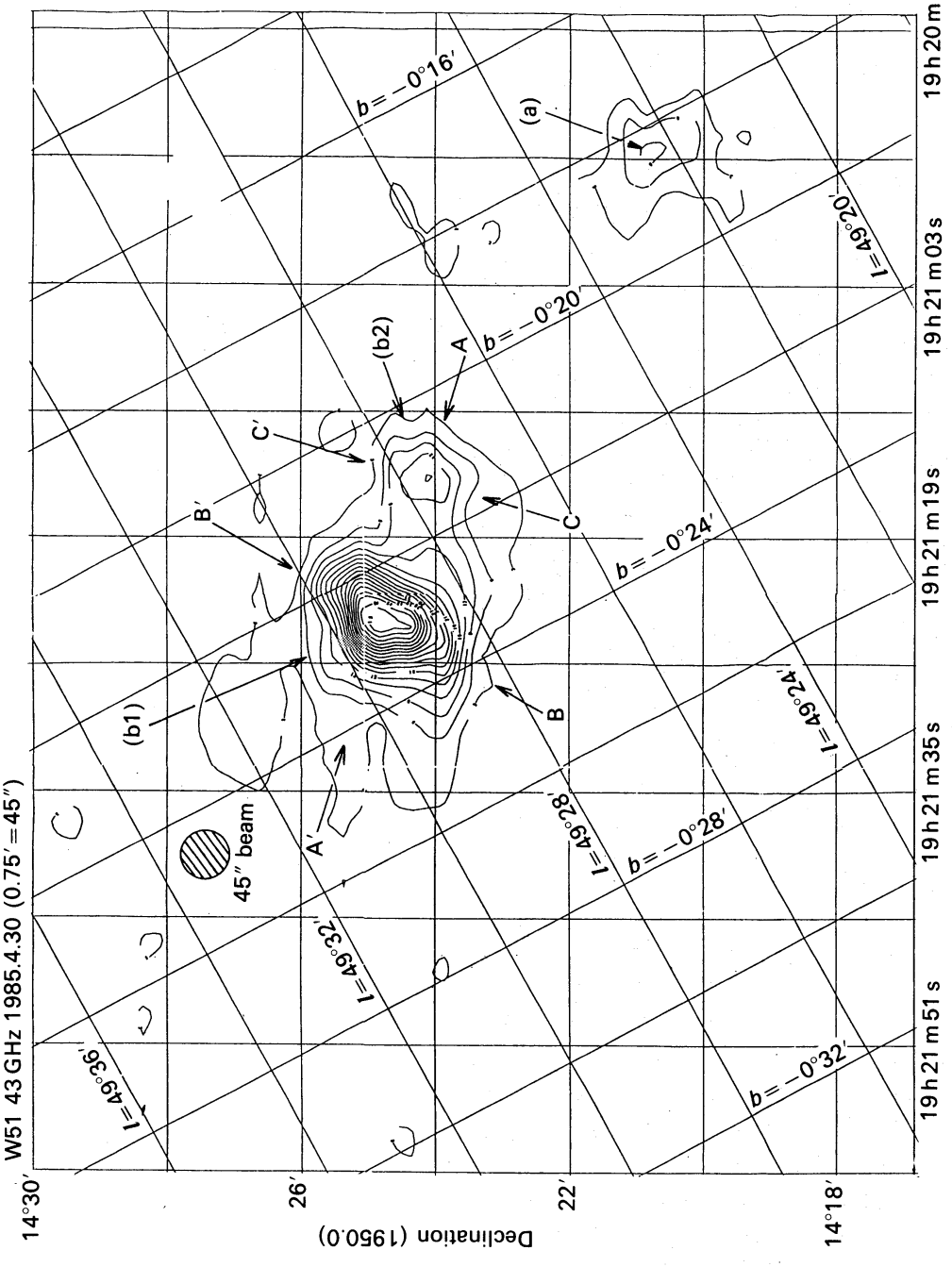

Fig. 5. 43.3-GHz map of W51 A. The top contour of the map corresponds to 8.7 K (±0.5 K) of the source T_B (brightness temperature). Arrows and indications such as AA′ show the cross-cut positions through the contour map. Components W51 (a), W51 (b1), and W51 (b2) are shown.

Table 3. Summary of the observational results of W51 A.

	W51 (a)		W51 (b1)		W51 (b2)		Total	
Peak position at 43.3 GHz								
R.A. (1950.0)	$19^h20^m55^s$		$19^h21^m25^s$		$19^h21^m16^s$		...	
Decl. (1950.0)	$+14°21'00''$		$+14°24'40''$		$+14°24'10''$		...	
Frequency (GHz) ..	84.2	43.3	84.2	43.3	84.2	43.3	84.2	43.3
S_ν (Jy)	15.5	15 ± 5	84.0	79 ± 10	...	12 ± 4	99.5	106 ± 15
				Source size θ_s				
Cross-cut:								
AA'	...	...	1'.02*	0'.75	~0'.5	0'.62	...	...
BB'	...	...	1'.45	1'.51	...	...	...	...
CC'	...	...	...	...	1'.13*	0'.73	...	...
... .	...	~0'.9 × ~0'.9	...	...	...	...	...	...

The 84.2-GHz results of Gordon et al. (1986) are also reproduced in the table for a comparison with the present work. AA' etc. in the table are marked in figure 5, showing the position of each cross-cut through the source.

Beamwidth: 70" at 84.2 GHz (Gordon et al. 1986) and 45" at 43.3 GHz.

hydrogen.

The 43.3-GHz structure of the region is quite consistent with the high-resolution interferometer results (Löbert and Goss 1978; Matthews et al. 1979; Felli et al. 1984) and also with the single-dish results (Lada et al. 1976; Gordon et al. 1986). Both the S- and N-bar regions essentially have a thermal spectra, as expected. However, we may propose here the possible existence of a 94.2-GHz excess emission relative to that at 43.3 GHz in the M17 (a2) area; the excess peak brightness is about 10% of the 94.2-GHz S-bar peak. This excess emission must come from extremely high-density and small-size electron condensations, which are still optically thick, even at 94.2 GHz. The area M17 (a2) shown in figures 1 and 3 seems to lie in a highly optically obscured region, and also seems to coincide with a separate velocity area of $+20\,\mathrm{km\,s^{-1}}$ in the red component of M17, observed by Gull and Balick (1974) with the H76α recombination lines. This sort of millimeter wave excess emission has already been discussed for the regions of Ori A and W3 by Akabane et al. (1985, 1986).

On the other hand, we have compared the present 43.3-GHz contour map of M17 with the Fleurs 1.415-GHz result (Löbert and Goss 1978). The 1.4-GHz half widths along the minor axes are appreciably narrower than those of 43.3 GHz, as indicated by asterisks in table 1, though the widths along the major axes are almost the same at the two frequencies. An example of a cross-cut comparison for both frequency maps is given in figure 6, where it can be seen that the width of the 1.4-GHz cross-cut is narrower than that of 43.3-GHz cross-cut. This may suggest that a brightness increase at 43.3 GHz relative to those at 1.4 GHz is more effectively observed at the edge of the source. When we assume a uniform electron temperature throughout the region, this may lead to the suggestion that some optically thick unfilled ionized clouds may exist

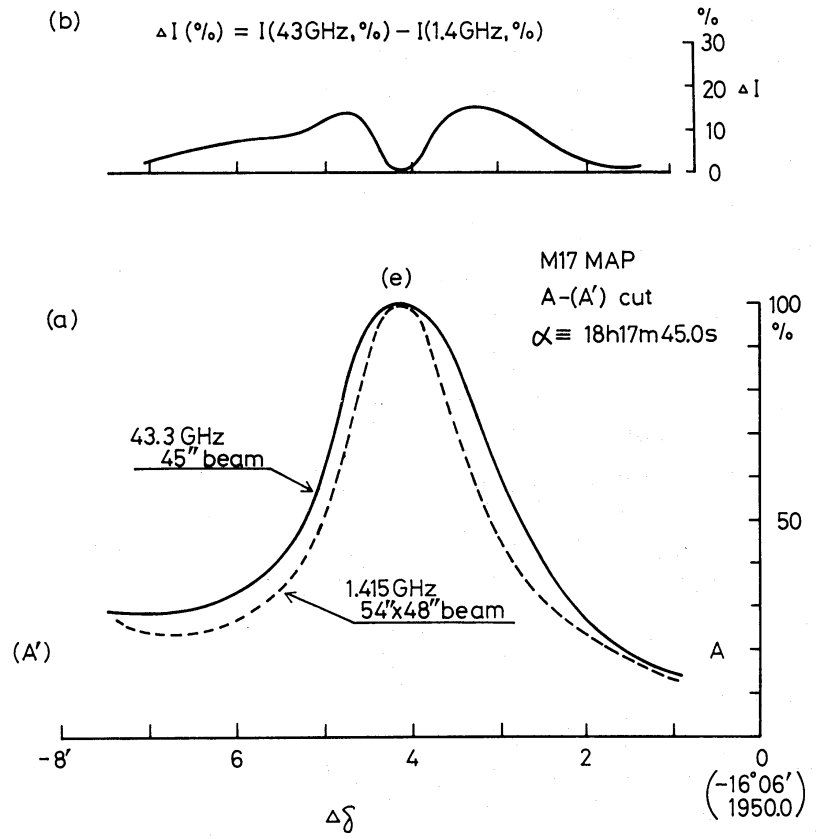

Fig. 6. 1.415- and 43.3-GHz cross-cuts through the peak (e), according to figure 1 of Löbert and Goss (1978), being along the AA′ cut in figure 3. Both are normalized at each cross-cut peak. (a) The lower figure is for the comparison of the cross-cut widths at 1.415 GHz (broken line) and 43.3 GHz (solid line), and (b) the upper figure is for a difference of the relative brightness between the two cross-cut profiles.

at both sides of the source, whereas the central part of the source remains optically thin even at this low frequency. A very wide distributed turn-over point ranging from 1 to 10 GHz for the thermal spectrum of M17, as summarized by Downes et al. (1970), may be attributed to this sort of complex structure of the optical thickness in this region. A qualitative study on this narrow width of the source structure at a frequency as low as 1.4 GHz will be presented in a forthcoming paper, along with a critical check of the Fleurs interferometer results.

4.2. W49 A and W51 A

W49 A was first resolved using the Cambridge One-mile radio telescope (Wynn-Williams 1969) as A_{51} and A_{59} at 1407 MHz. Schraml and Mezger (1969) observed a hardly resolved W49 A at 1.95 cm. Many observations between 5 and 15 GHz were reported, indicating a reasonable thermal spectrum of the source. Recently Gordon et al. (1986) made a 84.2-GHz observation and obtained a thermal flux density of 45.0 Jy for W49 A (table 2). The flux densities of the resolved components of W49 (a) and W49 (b), as denoted by Gordon et al. (1986), at 43.3 and 84.2 GHz can be compared with the interferometer results at 1407 MHz (Wynn-Williams 1969), where the flux

densities of each component are 25 and 8 Jy, respectively. We therefore know that each component of W49 A and W49 (b) also has an optically thin thermal spectrum over a wide range of frequencies down to 1407 MHz. A faint millimeter-wave excess emission has been proposed in the elongated area of (a′) in figure 4.

W51 A was resolved into W51 (a) and W51 (b), as denoted by Gordon et al. (1986), with single-dish observations by many workers from decimeter to short centimeter wavelength (Gardner and Morimoto 1968; Schraml and Mezger 1969; Shaver 1969; Goss and Shaver 1969; Shaver and Goss 1970; Altenhoff et al. 1978; Handa 1987). All of those showed a good thermal spectrum with an intensity of about 80 Jy and 15 Jy for the two components, respectively, though some high intensities were reported in the Australian observations. Gordon et al. (1986) made a short millimeter-wave (84.2 GHz) observation of the region and obtained reasonable thermal spectral intensities for each component (table 3).

In figure 5, we clearly resolve the sources W51 (b1) and W51 (b2), and also we note some elongaterd structure of W51 (b1). W51 (b) is also resolved in the 84.2-GHz map by Gordon et al. (1986). These structures are in good coincidence with the One-mile interferometer 2.7- and 5-GHz results by Martin (1972). Martin (1972) observed, the 2.7-GHz flux densities of about 50 Jy and 10 Jy for W51 (b1) and (b2), respectively. This, in comparison with those in table 3, may imply that each source of W51 (b1) or W51 (b2) is optically thin through a range down to 2.7 GHz or lower.

W51 (b1) had also been resolved by Scott (1978) at 5 GHz with the high-resolution Cambridge 5-km telescope into W51 main and W51 north components. Subsequent, 20- and. 8-μm observations by Genzel et al. (1982) also revealed the infrared fine structure of the W51 (b1) area. The elongation of the 43-GHz map of W51 (b1), as shown in figure 5, is quite consistent with these high-resolution results.

In figure 7, the two maps of W49 A and W51 (b) are reproduced with the sources located at the same distance: the map of W51 (b) is rotated, as indicated by α and δ in the figure, to show the similarity between the W49 A and the W51 (b) contours. To do this we adopted distances of 14.1 kpc (Akabane and Kerr 1965; Sato et al. 1967; Georgelin and Georgelin 1976) and 5.8 kpc (Georgelin and Georgelin 1976) to the W49 A and W51 (b) sources, respectively. The two maps shown in figure 7 indicate a morphological similarity to each other in the way that W49 (a) and (b) correspond to W51 (b1) and (b2), respectively, even though the absolute total intensities, n^2V, of the sources are quite different, (n is the electron density and V is the volume of the source). The n^2V of W49 A and W51 (b) are about 120- and 40-times as large as that of Ori A, respectively, as noted in the figure, showing that both sources are huge galactic H II regions.

5. Conclusions

43.3-GHz continuum maps of the M17, W49 A, and W51 A regions obtained with the NRO 45-m telescope were compared with other results. A morphological study was made for each source component with a high resolution of about 60″; each resolved component of the sources showed essentially a good optically thin thermal spectrum over a wide range of frequencies, down to 1.4 GHz. The localized spectral fine structure

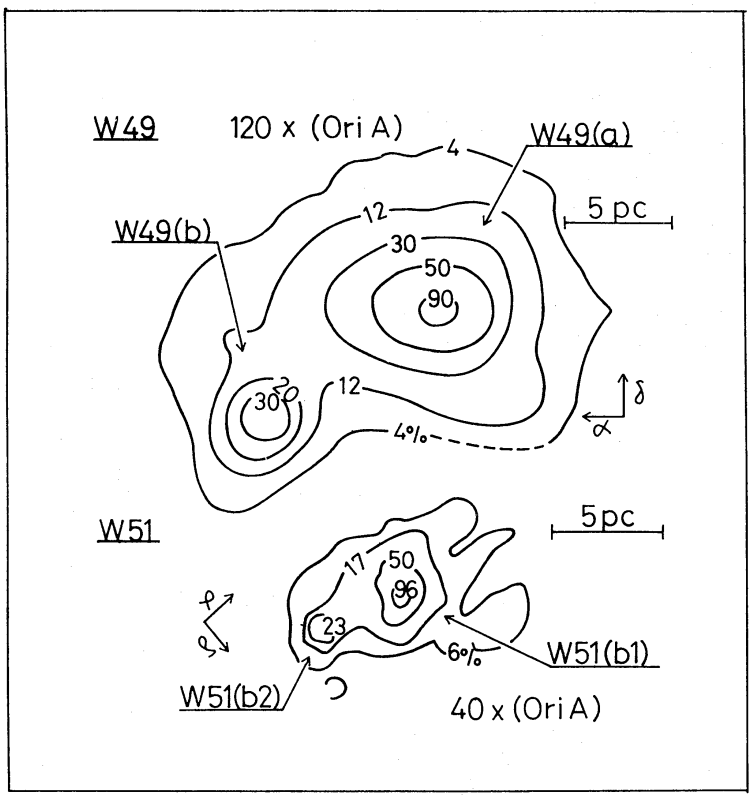

Fig. 7. 43.3-GHz brightness contours of W49 A and W51 (b). Two maps of the same linear scale, as they are put at the same distance, are shown with the relative brightness contour for each source.

in each region was also discussed, and the existence of optically thick components, even at 94.2 GHz, was suggested in the southern area of the M17 S-bar. The 43.3-GHz contour map was also compared with the Fleurs 1.4-GHz interferometer result, and an optically thick patchy structure surrounding each localized source of M17 has been proposed. The morphological similarity between W49 A and W51 (b) brightness features at the millimeter wave region is also shown.

We could examine the 23.2-GHz original map of M17 for a preliminary study thanks to the courtesy of Drs. W. Reich and P. Reich; this is greatly acknowledged. The authors are also grateful to the NRO engineers and operators for their collaboration and for the computer reduction, and to Miss A. Ide for her work on the drawings and the manuscript. The 43.3-GHz observations are part of the NRO continuum project, for which the Ori A, W3, and Sgr B2 regions have been reported (Akabane et al. 1985, 1986, 1988).

References

Akabane, K., Hirabayashi, H., and Sofue, Y. 1986, *Publ. Astron. Soc. Japan*, **38**, 775.
Akabane, K., and Kerr, F. J. 1965, *Australian J. Phys.*, **18**, 91.

Akabane, K., Sofue, Y., Hirabayashi, H., Inoue, M., Nakai, N., and Handa, T. 1985, *Publ. Astron. Soc. Japan*, **37**, 123.
Akabane, K., Sofue, Y., Hirabayashi, H., Morimoto, M., Inoue, M., and Downes, D. 1988, *Publ. Astron. Soc. Japan*, **40**, 459.
Altenhoff, W. J., Downes, D., Pauls, T., and Schraml, J. 1978, *Astron. Astrophys. Suppl.*, **35**, 23.
Downes, D., Maxwell, A., and Rinehart, R. 1970, *Astrophys. J. Letters*, **161**, L123.
Felli, M., Churchwell, E., and Massi, M. 1984, *Astron. Astrophys.*, **136**, 53.
Felli, M., Johnston, K. J., and Churchwell, E. 1980, *Astrophys. J. Letters*, **242**, L157.
Gardner, F. F., and Morimoto, M. 1968, *Australian J. Phys.*, **21**, 881.
Genzel, R., Becklin, E. E., Wynn-Williams, C. G., Moran, J. M., Reid, M. J., Jaffe, D. T., and Downes, D. 1982, *Astrophys. J.*, **255**, 527.
Georgelin, Y. M., and Georgelin, Y. P. 1976, *Astron. Astrophys.*, **49**, 57.
Gordon, M. A. 1987, *Atrophys. J.*, **316**, 258.
Gordon, M. A., Jewell, P. R., Kaftan-Kassim, M. A., and Salter, C. J. 1986, *Astrophys. J.*, **308**, 288.
Goss, W. M., and Shaver, P. A. 1970, *Australian J. Phys. Suppl.*, **14**, 1.
Gull, T. R., and Balick, B. 1974, *Astrophys. J.*, **192**, 63.
Handa, T. 1987, Ph. D. Dissertation, The University of Tokyo.
Harris, S., and Scott, P. F. 1976, *Monthly Notices Roy. Astron. Soc.*, **175**, 371.
Kleinmann, D. E. 1973, *Astrophys. Letters*, **13**, 49.
Lada, C. J., Dickinson, D. F., Gottlieb, C. A., and Wright, E. L. 1976, *Astrophys. J.*, **207**, 113.
Lemke, D., and Low, F. J. 1972, *Astrophys. J. Letters*, **177**, L53.
Löbert, W., and Goss, W. M. 1978, *Monthly Notices Roy. Astron. Soc.*, **183**, 119.
Martin, A. H. M. 1972, *Monthly Notices Roy. Astron. Soc.*, **157**, 31.
Matthews, H. E., Harten, R. H., and Goss, W. M. 1979, *Astron. Astrophys.*, **72**, 224.
Sato, F., Akabane, K., and Kerr, F. J. 1967, *Australian J. Phys.*, **20**, 197.
Schraml, J., and Mezger, P. G. 1969, *Astrophys. J.*, **156**, 269.
Scott, P. F. 1978, *Monthly Notices Roy. Astron. Soc.*, **183**, 435.
Shaver, P. A. 1969, *Monthly Notices Roy. Astron. Soc.*, **142**, 273.
Shaver, P. A., and Goss, W. M. 1970, *Australian J. Phys. Suppl.*, **14**, 133.
Sofue, Y., Inoue, M., Handa, T., Tsuboi, M., Hirabayashi, H., Morimoto, M., and Akabane, K. 1986, *Publ. Astron. Soc. Japan*, **38**, 475.
Sofue, Y., and Reich, W. 1979, *Astron. Astrophys. Suppl.*, **38**, 251.
Webster, W. J., Jr., Altenhoff, W. J., and Wink, J. E. 1971, *Astron. J.*, **76**, 677.
Wynn-Williams, C. G. 1969, *Monthly Notices Roy. Astron. Soc.*, **142**, 453.